



Preparation of Fully Synthetic Histone H3 Reveals That Acetyl-Lysine 56 Facilitates Protein Binding Within Nucleosomes

John C. Shimko¹, Justin A. North², Aaron N. Bruns¹,
Michael G. Poirier^{1,2,3*} and Jennifer J. Ottesen^{1*}

¹Department of Biochemistry and The Ohio State Biochemistry Program, The Ohio State University, Columbus, OH 43210, USA

²Department of Physics, The Ohio State University, Columbus, OH 43210, USA

³Department of Molecular Virology, Immunology, and Medical Genetics, The Ohio State University, Columbus, OH 43210, USA

Received 10 April 2010;

received in revised form

7 December 2010;

accepted 5 January 2011

Available online

15 February 2011

Edited by J. O. Thomas

Keywords:

nucleosome;

histone posttranslational

modification;

sequential native chemical

ligation;

fully synthetic histone;

histone H3 lysine 56

acetylation

Posttranslational modification (PTM) of histones plays a central role in genome regulation. Engineering histones with defined PTMs on one residue or on multiple residues is crucial for understanding their function within nucleosomes and chromatin. We introduce a sequential native chemical ligation strategy that is suitable for the preparation of fully synthetic histone proteins, allowing for site-specific incorporation of varied PTMs throughout the sequence. We demonstrate this method with the generation of histone H3 acetylated at lysine 56 [H3(K56ac)]. H3(K56ac) is essential for transcription, replication, and repair. We examined the influence of H3 (K56ac) on the targeting of a model DNA binding factor (LexA) to a site ~30 bp within the nucleosome. We find that H3(K56ac) increases LexA binding to its DNA target site by 3-fold at physiological ionic strength. We then demonstrate that H3(K56ac) facilitates LexA binding by increasing DNA unwrapping, not by nucleosome repositioning. Furthermore, we find that H3(K56Q) quantitatively imitates H3(K56ac) function. Together, these studies introduce powerful tools for the analysis of histone PTM functions.

© 2011 Elsevier Ltd. All rights reserved.

*Corresponding authors. M. G. Poirier is to be contacted at 191 West Woodruff, Columbus, OH 43210, USA; J. J. Ottesen, 484 West 12th Street, Columbus, OH 43210, USA. E-mail addresses: mpoirier@mps.ohio-state.edu; ottesen.1@osu.edu.

Abbreviations used: PTM, posttranslational modification; H3(K56ac), histone H3 acetylated at lysine 56; HO, histone octamer; NCL, native chemical ligation; FRET, fluorescence resonance energy transfer; Thz, thiazolidine; RP-HPLC, reverse-phase high-performance liquid chromatography; MALDI-TOF MS, matrix-assisted laser desorption ionization time-of-flight mass spectrometry; H3(C110A)_{syn}, synthetic H3(C110A); H3(C110A)_{rec}, recombinant H3(C110A); EDTA, ethylenediaminetetraacetic acid; FeBABA, Fe(III) (s)-1-(p-bromoacetamidobenzyl) ethylenediamine tetraacetic acid; EMSA, electrophoretic mobility shift assay; MESNA, sodium mercaptoethanesulfonate; GdnHCl, guanidinium hydrochloride; TFA, trifluoroacetic acid; TCEP, tris(2-carboxyethyl)phosphine; MPAA, 4-mercaptophenylacetic acid; BZA, benzamidine.

Introduction

Eukaryotic genomes are organized into long repeats of nucleosomes, which contain ~147 bp of DNA wrapped 1.65 times around H2A, H2B, H3, and H4 histone octamers (HOs).¹ DNA wrapped onto nucleosomes is sterically occluded from DNA interacting proteins,² yet this DNA must be accessed for gene expression, replication, and repair. The nucleosome undergoes thermal fluctuations that transiently unwrap nucleosomal DNA to expose it for protein interactions.^{2,3} The equilibrium between fully wrapped DNA and partially unwrapped DNA is termed "site exposure" and is greatest near the DNA entry–exit region of the nucleosome.² This property of the nucleosome appears to provide access to DNA processing proteins *in vivo*, such as photolyase access to damaged DNA within chromatin in budding yeast.⁴ In addition, adjacent DNA binding sites within a nucleosome display an inherent cooperativity^{5,6} that influences unwrapping and is likely to play an important role in genomewide transcriptional regulation.^{7,8}

Nucleosomes contain an enormous number of histone posttranslational modifications (PTMs) that appear to function singly and in different combinations⁹ to silence or activate wrapped nucleosomal DNA.¹⁰ PTMs on unstructured histone tails appear to function as binding modules for chromatin-associated proteins¹¹ and to influence higher-order chromatin structure.¹² In contrast, PTMs that reside within internal regions of the nucleosome are often inaccessible to binding partners¹³ but can directly alter inherent nucleosome structure and dynamics.^{14,15} Nucleosomes with well-defined PTMs are required to quantitatively determine the effect of these modifications on chromatin structure and dynamics, yet the preparation of such nucleosomes has posed a synthetic challenge.

Histones containing defined PTMs have recently been generated by expressed protein ligation, in which a single synthetic peptide that includes the desired modifications is ligated to an unmodified recombinant protein. This method has been generally limited to one or more modification types located near histone termini.^{12,14,16–19} Methylated and acetylated lysines have been introduced chemically as thioether-containing lysine analogs.^{20,21} More recently, methods have been introduced that exploit pyrrolyl-tRNA synthetase/tRNA_{CUA} pairs evolved for specific incorporation of acetylated or mono-methylated lysines into proteins. While these methods can be used to introduce this subset of modifications anywhere in a protein sequence, they are limited to the incorporation of a single modification type into each histone.^{15,22} However, a typical biologically relevant histone protein often contains multiple simultaneous PTMs throughout the histone sequence.²³ Here, we demonstrate a sequential native chemical ligation (NCL) strategy^{24–27} to prepare fully

synthetic histones. This opens up the possibility of preparing histones with any desired set of modifications. We applied this scheme to generate a full-length histone H3 acetylated at lysine 56 [H3(K56ac)].

H3(K56ac) is required for a number of DNA processes.^{28,29} H3(K56) appears to be acetylated prior to deposition onto newly replicated DNA³⁰ and is important for DNA repair,^{31,32} maintenance of genomic stability,³³ and transcriptional regulation.^{30,34,35} It has been suggested that H3(K56ac) alters chromatin structure and dynamics, allowing accessibility to DNA metabolic proteins³⁰ and acting as a signal to DNA damage checkpoints.³¹

The preparation of H3(K56ac) using the evolved pyrrolylincorporation machinery was reported recently.¹⁵ This study suggested that H3(K56ac) modestly increased SWI/SNF and RSC-catalyzed nucleosome repositioning, and increased DNA unwrapping at the entry–exit region. They also found that H3(K56ac) did not influence chromatin compaction. However, a separate study of the acetylation mimic H3(K56Q) found that it inhibited interactions between chromatin fibers.³⁶ Taken together with previous telomere studies, these results are consistent with the notion that H3(K56ac) may function in part as a DNA entry–exit gate for access to nucleosome DNA.^{15,35} Recently, it was also reported that H3(K56ac) reduces H3–H4 tetramer binding by the histone chaperone Nap1.³⁷ The direct nucleosome characterization in these studies provides a standard by which we may validate the utility of our synthetic strategy. In addition, the influence of H3(K56ac) on protein binding within the nucleosome remains a significant unknown.

Following the incorporation of a full-length fully synthetic H3(K56ac) into nucleosomes, we tested the DNA entry–exit gate hypothesis using a fluorescence resonance energy transfer (FRET) system to quantitatively detect protein binding to partially unwrapped nucleosomal DNA.³ We find that both H3(K56ac) and the acetyl-lysine mimic H3(K56Q) alter nucleosome equilibrium toward DNA unwrapping at the DNA entry–exit region. We also demonstrate that H3(K56ac) and H3(K56Q) increase the accessibility of a model DNA binding protein (LexA) to a target site 27 bp into the nucleosome. These results suggest that H3(K56ac) and H3(K56Q) shift the equilibrium of DNA site exposure to increase access of DNA metabolic proteins to DNA sites that are at least 27 bp within the nucleosome.

Results

Preparation of fully synthetic H3(R40C,K56ac,S96C,C110A) that contains two nonnative cysteines

Histone H3 is a 135-residue protein that can be easily refolded and incorporated into a nucleosome.

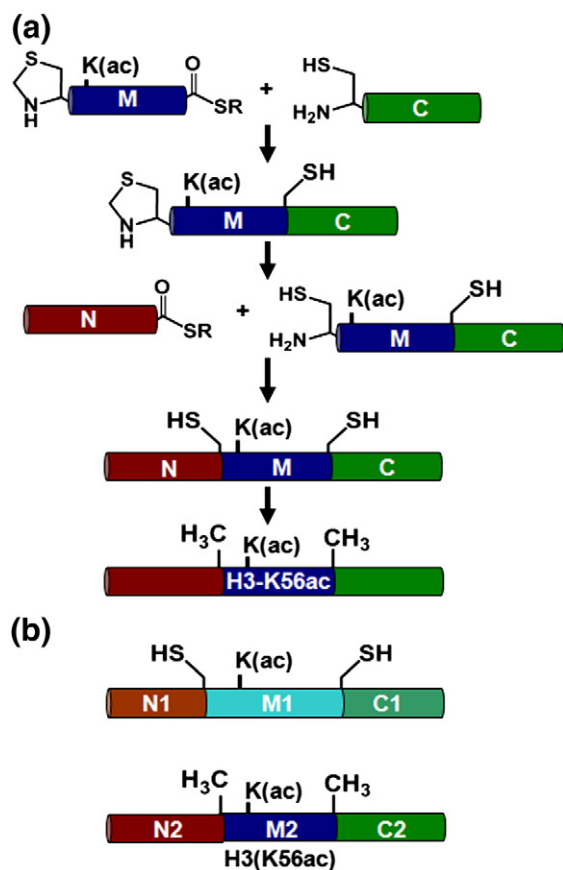


Fig. 1. Assembly of modified histone H3 by NCL used in the analysis of reconstituted nucleosomes. (a) Schematic representation of the total synthesis of H3(K56ac) using sequential NCL in solution phase. The synthesis of H3 (R40C,K56ac,S96C,C110A) proceeded through the second ligation step; the synthesis of H3(K56ac) used new ligation sites and added the final desulfurization step to generate the native sequence. (b) Proteins generated and characterized: H3(R40C,K56ac,S96C,C110A) and H3(K56ac,C110A).

This property makes it an excellent candidate for total synthesis by sequential NCL. As the basis for our ligation strategies, we selected the modified *Xenopus*

laevis H3(C110A) sequence, which is commonly used in biophysical studies.³⁸ The C110A substitution occurs in yeast and has not previously been reported to affect nucleosome structure, positioning, and DNA unwrapping.^{39,40}

NCL is the chemoselective reaction between a polypeptide containing an N-terminal Cys and a polypeptide containing a C-terminal thioester that ultimately generates a native peptide bond with a Cys at the ligation site. Cys residues were introduced into H3(C110A) at Arg40 and Ser96 based on homology alignments that found H3(R40C) in *Cairina moschata*⁴¹ and H3(S96C) in the H3.1 variants in *Homo sapiens*, *Mus musculus*,⁴² and *Caenorhabditis elegans*.⁴³ These Cys residues could be crafted into a two-step NCL strategy in which the longest synthetic segment would be a central 56-residue peptide containing an acetylated lysine that would eventually become Lys56 (Fig. 1a). In this strategy, the N-terminal and middle segments (N1 and M1; see Table 1) were synthesized with C-terminal thioesters. A key feature of the synthesis was the introduction of the N-terminal Cys in the middle segment M1 as a thiazolidine (Thz) moiety.^{24,44} After the first ligation step that linked the M1 and C1 peptides, the ligation mixture was treated with methoxylamine to unmask the N-terminal Cys of the M1C1 product prior to purification (Fig. 2a). This product was then reacted with peptide N1 to generate the full-length H3 (R40C,K56ac,S96C,C110A) (Figs. 1b and 2b). The purified histone showed evidence of methionine oxidation (see Supplemental Information), which required a methionine reduction step, followed by final purification and analysis (Fig. 2c and d). While each of the ligation steps proceeded to >70%, the three reverse-phase high-performance liquid chromatography (RP-HPLC) purification steps resulted in significant product loss. The full ligation pathway resulted in a yield of 48 μ g of H3(R40C,K56ac,S96C,C110A), which represents an overall yield of 2% based on the limiting central peptide. While these yields were low, they were sufficient for initial studies.

Table 1. Sequence of peptide segments utilized in each sequential ligation scheme

Peptide	Description	Sequence
N1	Unmodified H3(1–39) thioester	ARTKQTARKSTGGKAPRKQLATKAARKSAPATGGVKKPH-COSR
M1	H3(40–95) R40Thz,K56ac thioester	(Thz)YRPGTVLREIRRYQ(Kac)STELLIRKLPQRLVREIAQDFKTDLRFQSSAVMALQEA-COSR
C1	H3(96–135) S96C,C110A	CEAYLVALFEDTNLAAIHAKRVTIMPKDIQLARRIRGERA-COOH
N2	Unmodified H3(1–46) thioester	ARTKQTARKSTGGKAPRKQLATKAARKSAPATGGVKKPHRYRPGTV-COSR
M2	H3(47–90) A47Thz,K56ac thioester	(Thz)LREIRRYQ(Kac)STELLIRKLPFQRLVREIAQDFKTDLRFQSSAVM-COSR
C2	H3(91–135) A91C,C110A	CLQEASEAYLVALFEDTNLAAIHAKRVTIMPKDIQLARRIRGERA-COOH
M3	H3(47–90) A47Thz thioester	(Thz)LREIRRYQKSTELLIRKLPFQRLVREIAQDFKTDLRFQSSAVM-COSR

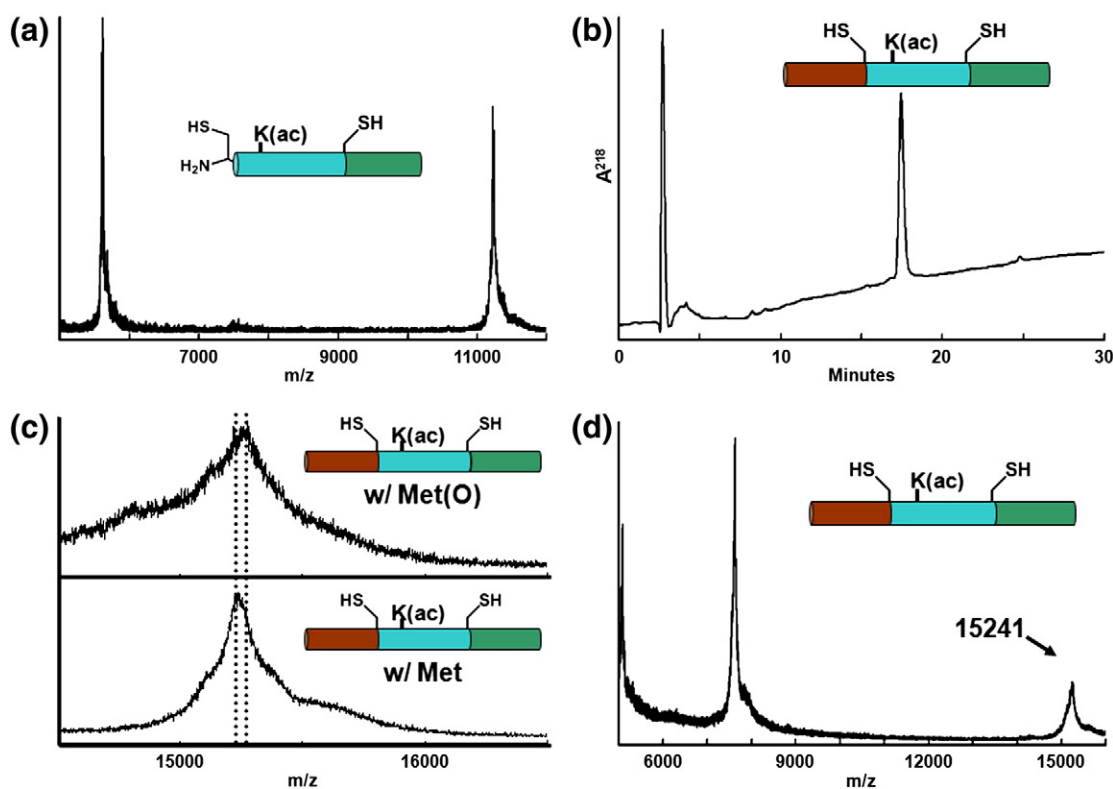


Fig. 2. Sequential NCL to generate H3(R40C,K56ac,S96C,C110A). (a) MALDI-TOF MS analysis of the first ligation product after Thz ring opening: residues 40–135 of H3(R40C,K56ac,S96C,C110A). A doublet of peaks corresponding to the Met and Met(O) species of the desired product was observed: Met, m/z expected, 11,221; m/z observed, 11,221; Met(O) species, m/z expected, 11,237; m/z observed, 11,237. (b) RP-HPLC of the final reduced H3(R40C,K56ac,S96C,C110A) with a gradient of 27–54% isopropanol/0.1% TFA at 45 °C. (c) Reduction of Met(O) to Met in the final ligation product H3(R40C,K56ac,S96C,C110A). Top: MALDI-TOF MS spectrum of the reduction mixture at 0 min, containing primarily H3(R40C,K56ac,S96C,C110A) Met(O) species (m/z expected, 15,256; m/z observed, 15,253). Bottom: MALDI-TOF MS spectrum of the reduction mixture at 60 min, containing primarily H3(R40C,K56ac,S96C,C110A) Met species (m/z expected, 15,240; m/z observed, 15,237). (d) MALDI-TOF MS of reduced H3(R40C,K56ac,S96C,C110A) (m/z expected, 15,240; m/z observed, 15,241).

The introduction of nonnative cysteines in histone H3 alters nucleosome structure

The first-generation synthetic H3 retained a Cys at each ligation site. Nucleosomes were reconstituted (Fig. 3) with a 5'-Cy3-end-labeled 147-bp 601 nucleosome positioning sequence containing a LexA binding site located between 8 bp and 27 bp (Fig. 3a, 601-LexA-end), and HOs containing Cy5-labeled H2A(K119C) (Fig. 3b) with either unmodified H3, H3(R40C,S96C,C110A), H3(R40C,K56Q,S96C,C110A), or synthetic H3(R40C,K56ac,S96C,C110A), and purified on a sucrose gradient. Following reconstitution, the Cy3 and Cy5 FRET pairs were juxtaposed near the entry–exit region of the nucleosome (Fig. 3b, green and magenta).³ The placement of one fluorophore on the DNA and of the other fluorophore on the HO allows the detection of DNA movement relative to the HO. Unfortunately, we found that the FRET efficiency decreased from 0.62 ± 0.02 to 0.43 ± 0.01 when wild-type H3-containing

nucleosomes were compared to the control H3(R40C,S96C,C110A)-containing nucleosomes (Fig. 4). This observation suggests that the H3(R40C,S96C)-containing nucleosomes display altered structure and/or dynamics. Nucleosomes containing H3(R40C,K56Q,S96C,C110A) or H3(R40C,K56ac,S96C,C110A) resulted in a further decrease in FRET efficiency to 0.38 ± 0.02 and 0.35 ± 0.04 , respectively (Fig. 4c). However, this additional reduction in FRET efficiency is significantly less than that induced with the Cys substitutions alone. Our results reveal the potential pitfalls associated with the introduction of nonnative histone sequence substitutions in nucleosome structure and/or dynamics.

Preparation of fully synthetic wild-type histones H3(K56ac,C110A) and H3(C110A)

Because the introduction of nonnative Cys residues significantly influenced nucleosome structure and/or dynamics, we improved our method for

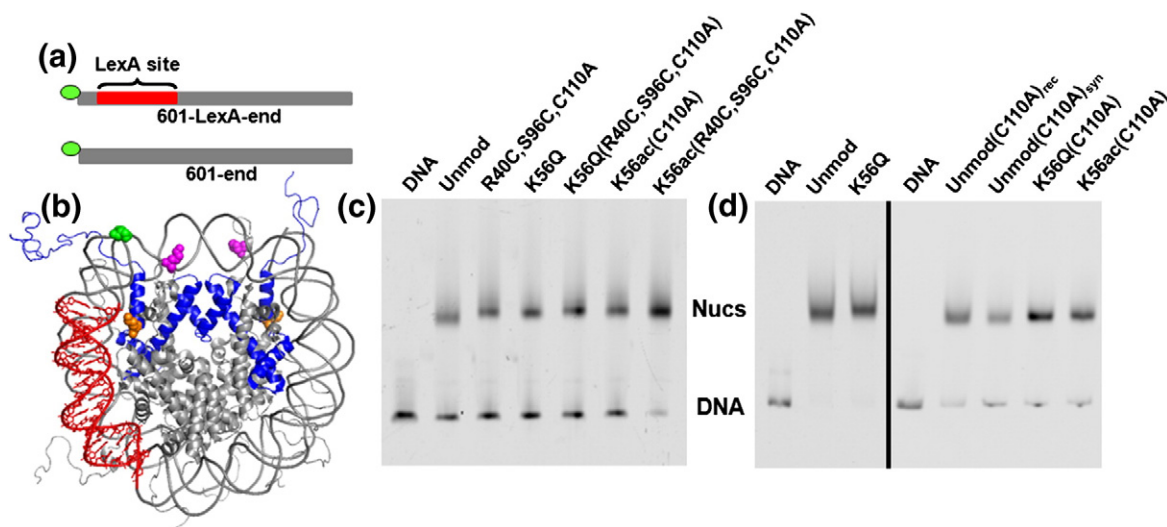


Fig. 3. DNA substrates and reconstituted nucleosomes containing Cy3 and Cy5 for FRET measurements. (a) The 147-bp DNA molecules 601-LexA-end and 601-end contain the 601 positioning sequence with and without a LexA binding site at base pairs 8–27, respectively, and a Cy3 fluorophore attached to the 5' end. (b) Structure of the nucleosome reconstituted for FRET analysis.⁴⁵ Histone H3 is depicted in blue ribbons, with K56 highlighted in orange. Histone H2A(K119C) (magenta) has been modified with Cy5. A DNA construct specifically labeled at the first base with Cy3 (green) and containing a LexA binding site (red). (c and d) Cy3 fluorescence images of a PAGE analysis of nucleosome reconstitutions before and after purification by sucrose gradient centrifugation, respectively.

preparing fully synthetic native histones containing defined PTMs. In this second-generation approach, we combined sequential NCL with a desulfurization step⁴⁷ (Fig. 1a). This scheme allows the more common Ala residue to be used as a ligation site. We selected the native Ala residues H3(A47) and H3(A91) and synthesized three peptides (N2, M2, C2; see Table 1). The H3(A47) residue was incorporated as Thz (peptide M2), and H3(A91) was incorporated as Cys (peptide C2), to allow sequential ligation (Fig. 1). Peptide M2 was mixed with an excess of peptide C2 to form the ligation product M2C2 that was purified by RP-HPLC (Fig. 5a). Ring opening of Thz was subsequently carried out on the product using methoxylamine to reveal the N-terminal Cys (Fig. 5b). The order of ring opening and purification minimized the reformation of Thz by trace amounts of aldehyde that copurify with the N2 peptide, which renders M2C2 inactive (see Materials and Methods). Peptide N2 was added directly to the mixture, and buffer conditions were adjusted to initiate ligation. Ligation was allowed to proceed for at least 4 days until no further product formation was observed (Fig. 5c). Free-radical desulfurization⁴⁷ was carried out directly on the crude ligation mixture to convert the ligation site Cys into the Ala found in the native H3 sequence. Desulfurization was monitored by matrix-assisted laser desorption ionization time-of-flight mass spectrometry (MALDI-TOF MS) (Fig. 5d). H3(K56ac, C110A) was purified by RP-HPLC (Fig. 5e), and the product was lyophilized for subsequent refolding into nucleosomes. A

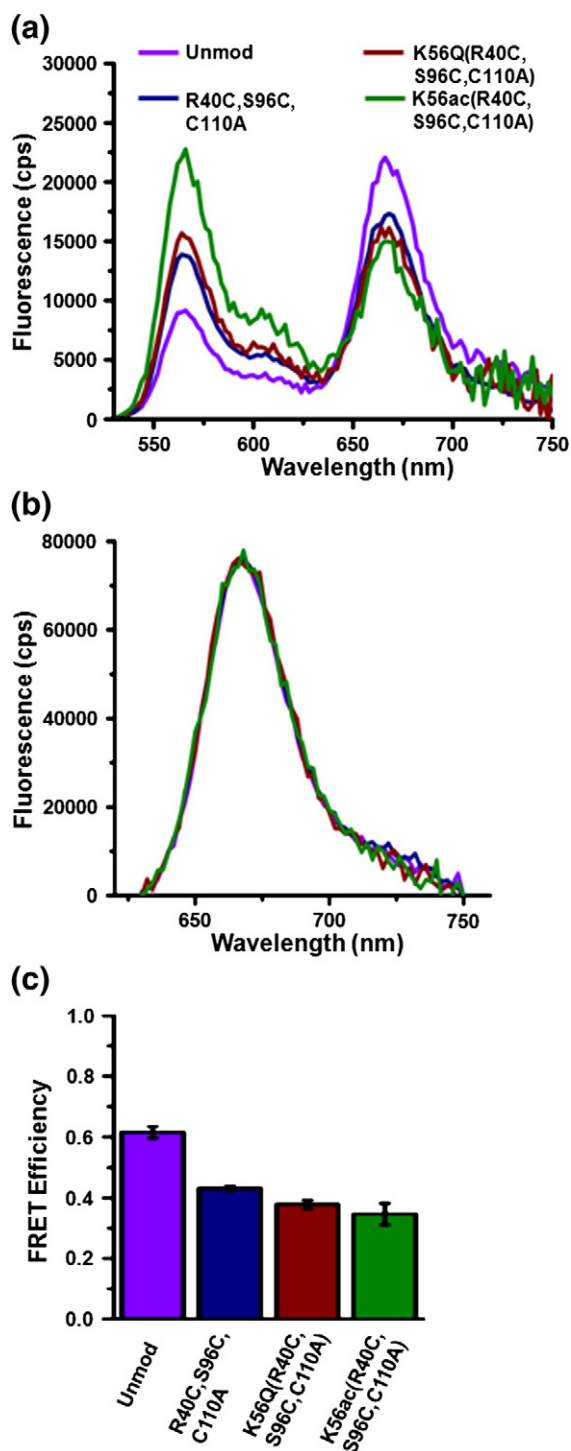
typical ligation cycle produced 93 μg of H3(K56ac, C110A) at >95% purity, with 500 μg of peptide M2 as limiting reagent. This corresponds to an overall yield of 7% through all synthetic steps. This new scheme provides a reproducible 3-fold increased yield over the original synthetic pathway, allowing us to generate over 0.5 mg of the native histone suitable for detailed biophysical characterization. Moreover, the only limitation to preparing virtually any PTM or any combination of PTMs on any histone would appear to be the ability to synthesize appropriately modified ligation peptides.

We repeated the sequential ligation using the synthetic segment M3, which bears the unmodified K56 residue, to generate 120 μg of synthetic H3 (C110A) [H3(C110A)_{syn}] (Fig. 5f). Nucleosomes containing this synthetic unmodified protein were directly compared to nucleosomes reconstituted with recombinant H3(C110A) [H3(C110A)_{rec}] to demonstrate that the synthetic process did not introduce any undesired modifications.

Acetylation of H3(K56) reduces DNA wrapping at the entry–exit region of the nucleosome

We examined the biophysical properties of H3 (K56ac) and H3(K56Q) using the FRET system described above (Fig. 3a, 601-LexA-end). We determined the FRET efficiency at low ionic strength [0.5 \times TE buffer with 1 mM Na⁺ from disodium ethylenediaminetetraacetic acid (EDTA)] for nucleosomes containing unmodified H3, H3(K56Q), H3

(C110A)_{rec}, H3(C110A)_{syn}, H3(K56Q,C110A), and H3(K56ac,C110A), and at physiological ionic strength (0.5× TE buffer with 75 mM or 130 mM NaCl) for nucleosomes containing H3(C110A)_{rec}, H3(C110A)_{syn}, H3(K56Q,C110A), and H3(K56ac,C110A) (Fig. 6, Table 2). We find that the FRET efficiency is reduced by about 15–20% for nucleosomes containing H3(K56ac,C110A), H3(K56Q), and H3(K56Q,C110A).



In contrast, the FRET efficiency is increased by 6% with H3(C110A)_{rec} and is unaltered for H3(C110A)_{syn} with respect to unmodified H3 (Fig. 6c). These results indicate that H3(K56ac) increases the average distance between the DNA and the histone surface at the entry–exit region under low and physiological ionic strengths. In addition, H3(K56Q) appears to quantitatively mimic the effects of H3(K56ac) on the steady-state structure, and this difference does not depend on ionic strength.

Nucleosomes containing H3(K56ac) or H3(K56Q) showed a slight shift in electrophoretic mobility. Altered mobility could be explained by the increase in DNA unwrapping, consistent with our FRET measurements; alternatively, it could be attributed to a shift in nucleosome position. We therefore determined the positions of nucleosomes containing H3(C110A)_{rec} and H3(K56Q,C110A) by hydroxyl radical cleavage³⁹ using Fe(III) (s)-1-(p-bromoacetamidobenzyl) ethylenediamine tetraacetic acid (FeBABE); this label did not alter the gel mobility of nucleosomes containing H3(C110A)_{rec} or H3(K56Q,C110A) (Fig. 7b). We found that the cleavage pattern was indistinguishable between these nucleosomes (Fig. 7c and d). This indicates that the observed altered mobility and reduced FRET of nucleosomes containing H3(K56Q) and, by extension, H3(K56ac) are not due to nucleosome repositioning but rather due to increased DNA unwrapping.

Acetylation of H3(K56) facilitates protein binding within the nucleosome at low ionic strength

We initially determined the influence of H3(K56ac) and H3(K56Q) on DNA unwrapping and protein binding to a DNA target site buried within the nucleosome at low ionic strength, since previous FRET studies of DNA unwrapping have been carried out under these conditions.^{3,15,48–50} We performed LexA binding studies³ by detecting the reduction in FRET efficiency that is due to LexA binding to its target sequence, which is located within the nucleosome between base pairs 8 and 27 of the 147-bp 601 nucleosome positioning sequence (Figs. 3a and 8a–c). We initially titrated LexA from 0 μ M to 3 μ M in the

Fig. 4. FRET efficiency and LexA binding are impacted by cysteines introduced in H3, in addition to H3(K56Q) and H3(K56ac). (a) Fluorescence emission spectrum from nucleosomes containing unmodified H3 (purple), H3(R40C,S96C,C110A) (blue), H3(R40C,K56Q,S96C,C110A) (red), or H3(R40C,K56ac,S96C,C110A) (green) when excited at 510 nm (donor excitation). (b) Fluorescence emission spectrum from nucleosomes in (a) when excited at 610 nm (acceptor-only excitation). (c) The energy transfer efficiency for nucleosomes containing unmodified H3, H3(R40C,S96C,C110A), H3(R40C,K56Q,S96C,C110A), or H3(R40C,K56ac,S96C,C110A) determined from the (ratio)_A method.⁴⁶ The error bars were determined from the standard deviation of at least three separate measurements.

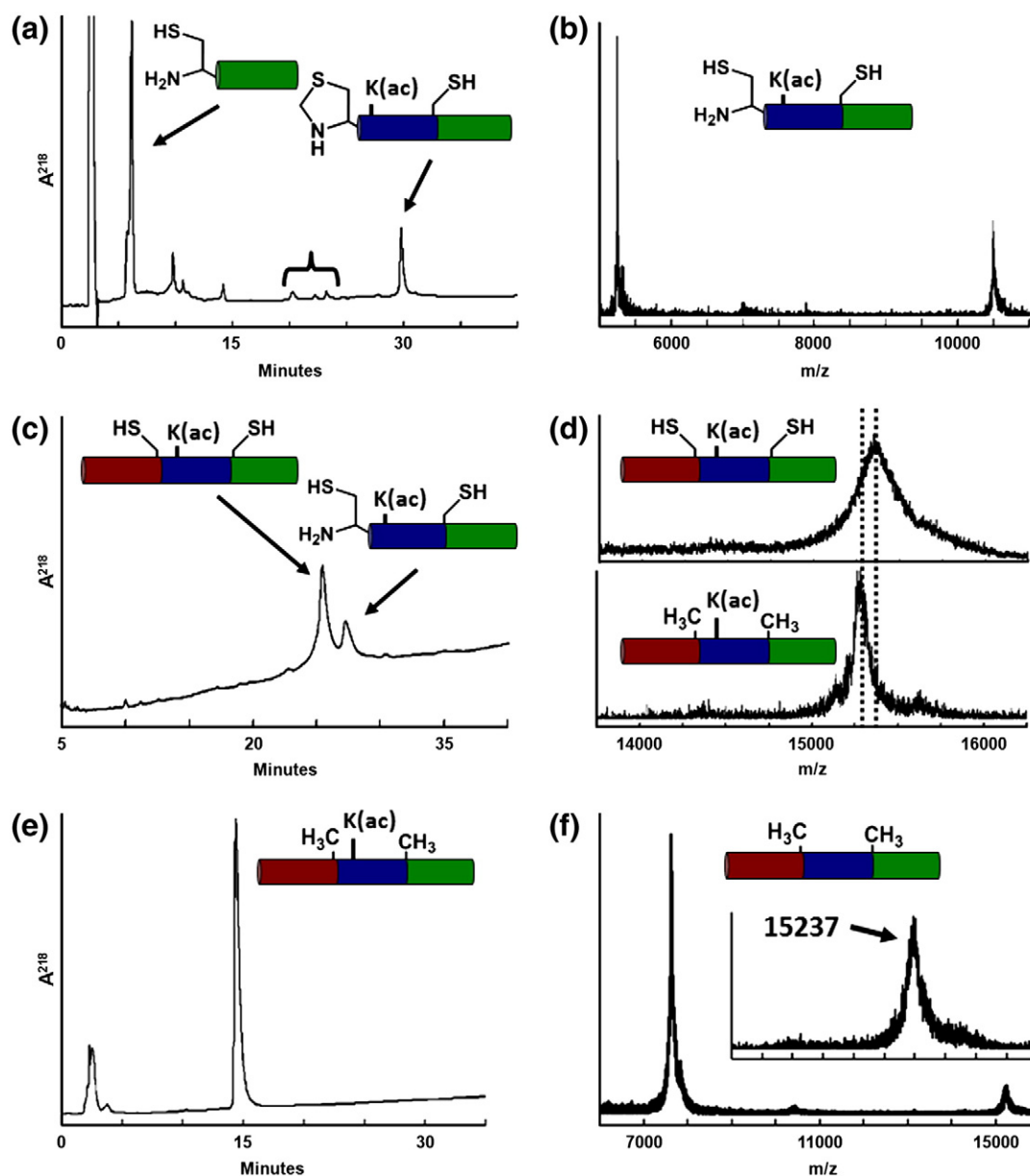


Fig. 5. Sequential NCL to generate synthetic H3(K56ac,C110A). (a) RP-HPLC chromatogram of a reaction mixture to generate the first ligation product: residues 47–135 of H3(A47Thz,K56ac,A91C,C110A) (gradient of 27–66% acetonitrile/0.1% TFA). (b) MALDI-TOF MS analysis of the first ligation product: m/z expected, 10,491; m/z observed, 10,492. (c) RP-HPLC of the second ligation step to generate H3(A47C,K56ac,A91C,C110A) (gradient of 41–59% acetonitrile/0.1% TFA). (d) Top: MALDI-TOF MS analysis of synthetic H3(A47C,K56ac,A91C,C110A) prior to desulfurization (m/z expected, 15,342; m/z observed, 15,338). Bottom: Final product H3(K56ac,C110A) (m/z expected, 15,278; m/z observed, 15,280). (e) RP-HPLC of synthetically generated H3(K56ac,C110A) with a gradient of 43–61% acetonitrile/0.1% TFA gradient. (f) MALDI-TOF MS analysis of H3(C110A)_{syn} (m/z expected, 15,236; m/z observed, 15,237). Inset: Magnified view with scale set as in (d).

presence of 1.0 mM Na⁺ and found that the FRET efficiency reduces to approximately 0.2 at high concentrations of LexA (Fig. 8d). Such a nonzero FRET efficiency at high LexA concentrations is concordant with previous site accessibility measurements.³ These results are consistent with the conclusion that unmodified nucleosomes and

nucleosomes containing H3(K56ac) or H3(K56Q) are not disassembled by LexA binding.

The FRET efficiencies in the presence of LexA were fitted to a noncooperative binding curve, and the concentration of half-saturation by LexA ($S_{0.5-nuc}$) was determined for nucleosomes containing unmodified H3, H3(K56Q), H3(C110A)_{rec}, H3(C110A)_{syn}, H3

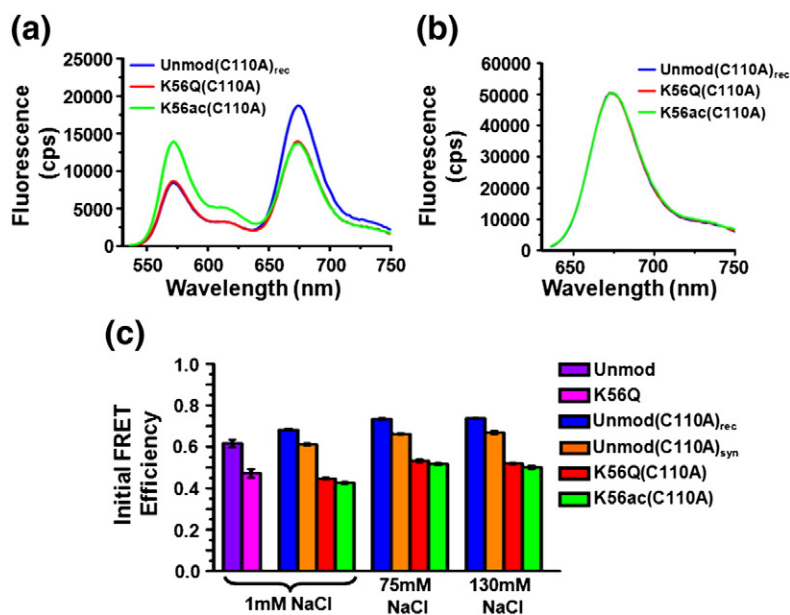


Fig. 6. FRET efficiency is reduced by H3(K56Q) and H3(K56ac). (a) Fluorescence emission spectra from nucleosomes containing unmodified H3(C110A) (blue), H3(K56Q,C110A) (red), and H3(K56ac,C110A) (blue) when excited at 510 nm (donor excitation) with 130 mM NaCl. (b) Fluorescence emission spectrum from nucleosomes in (a) when excited at 610 nm (acceptor excitation). (c) The FRET efficiency, as determined by the $(ratio)_A$ method,⁴⁶ of nucleosomes containing unmodified H3 (purple) and H3(K56Q) (magenta) at 1 mM NaCl, and unmodified H3 (C110A)_{rec} (blue), unmodified H3 (C110A)_{syn} (orange), H3(K56Q, C110A) (red), and H3(K56ac,C110A) (green) at 1 mM, 75 mM, and 130 mM NaCl. The error bars were determined from the standard deviation of three separate measurements.

(K56Q,C110A), and H3(K56ac,C110A) (Fig. 8d and e, Table 2). The concentration of half-saturation by LexA binding to its site within naked DNA was determined by gel shift analysis.³ We used two separate preparations of LexA with $S_{0.5-DNA}$ values of 0.14 ± 0.02 nM and 0.32 ± 0.04 nM (see Supplemental Information).

We determined the site exposure equilibrium constant K_{eq} from the half-saturation value of LexA binding to its target sequence within the nucleosome and to naked DNA, since $S_{0.5-nuc} = S_{0.5-DNA} / K_{eq}$ in the limit that K_{eq} is much less than 1 (see Materials and Methods for details). From this equation, we determined the equilibrium constant for site exposure for nucleosomes containing unmodified H3, H3(K56Q), H3(C110A)_{rec}, H3(C110A)_{syn}, H3(K56Q, C110A), and H3(K56ac,C110A) (Fig. 8f, Table 2) at low ionic strength (1 mM Na⁺).

We confirmed by electrophoretic mobility shift assays (EMSAs) that the reduction in FRET efficiency is due to LexA binding (see Supplemental Information). We find, as previously reported,³ that the LexA–nucleosome complex is not stable under

electrophoretic conditions. Therefore, we used glutaraldehyde to cross-link the LexA–nucleosome complex to prevent dissociation. We find that $S_{0.5-nuc}$, as determined by EMSA, is consistent with the measured reduction of FRET efficiencies for nucleosomes containing H3(C110A)_{rec}, H3(K56Q, C110A), and H3(K56ac,C110A). Furthermore, the increase in K_{eq} by H3(K56Q,C110A) and H3(K56ac, C110A), as measured by EMSA, is consistent with the increased K_{eq} determined by FRET efficiency measurements.

We controlled for the effects of nonspecific LexA binding on FRET efficiency by determining the FRET efficiency of nucleosomes that did not contain the LexA target sequence (Fig. 3a, 601-end). We find no decrease in the FRET efficiency in the presence of up to 1 μ M LexA (see Supplemental Information). This concentration of LexA fully reduces the FRET efficiency of nucleosomes that contain the LexA target sequence (Fig. 8d and e). These results confirm that the reduction in the FRET efficiency is due to LexA binding to its target sequence within the nucleosome.

Table 2. The FRET efficiency without LexA (E_0), the concentration of half-saturation by LexA to the nucleosome ($S_{0.5-nuc}$), the nucleosome site exposure equilibrium constant of the LexA target site (K_{eq}), and the relative nucleosome site exposure equilibrium constant with respect to recombinant H3 or H3(C110A)_{rec} (K_{eq-rel})

H3 histone	1 mM Na ⁺				75 mM NaCl			130 mM NaCl		
	E_0	$S_{0.5-nuc}$ (nM)	K_{eq}	K_{eq-rel}	E_0	$S_{0.5-nuc}$ (nM)	K_{eq-rel}	E_0	$S_{0.5-nuc}$ (nM)	K_{eq-rel}
H3	0.62 ± 0.02	43 ± 3	0.0033 ± 0.0005	1	—	—	—	—	—	—
H3(K56Q)	0.47 ± 0.02	22 ± 2	0.0063 ± 0.0010	1.9 ± 0.4	—	—	—	—	—	—
H3(C110A) _{rec}	0.68 ± 0.01	58 ± 6	0.0056 ± 0.0009	1	0.73 ± 0.01	3240 ± 181	1	0.74 ± 0.01	13,122 ± 536	1
H3(C110A) _{syn}	0.61 ± 0.01	62 ± 7	0.0052 ± 0.0008	0.9 ± 0.2	0.66 ± 0.01	—	—	0.67 ± 0.01	11,849 ± 876	1.1 ± 0.2
H3(K56Q,C110A)	0.45 ± 0.01	32 ± 3	0.0102 ± 0.0014	1.8 ± 0.4	0.53 ± 0.01	1276 ± 150	2.5 ± 0.6	0.52 ± 0.01	5176 ± 524	2.5 ± 0.5
H3(K56ac,C110A)	0.43 ± 0.01	32 ± 3	0.0102 ± 0.0015	1.8 ± 0.4	0.52 ± 0.01	991 ± 115	3.3 ± 0.7	0.50 ± 0.01	3975 ± 488	3.3 ± 0.7

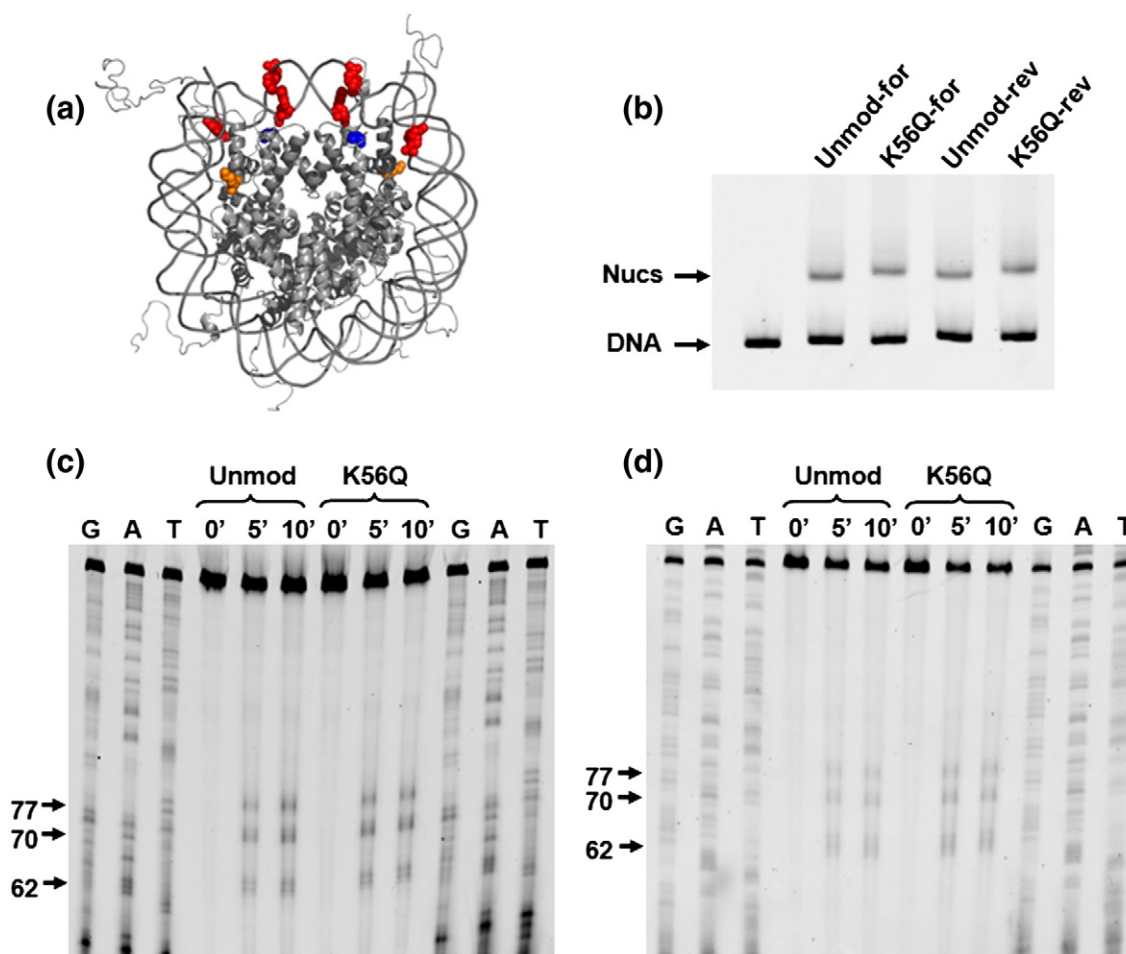


Fig. 7. Nucleosome positioning is not influenced by K56Q. (a) The crystal structure of the nucleosome with H3(K56) (orange), H4(S47), which is replaced with a cysteine and labeled with FeBABLE (blue), and the bases that are cleaved by FeBABLE (red). (b) EMSA of nucleosomes labeled with FeBABLE at H4(S47C). Lane 1 contains the DNA substrate. Lanes 2 and 4 contain nucleosomes with H3(C110A)_{rec}, with the top and bottom DNA strands 5' labeled with Cy3, respectively. Lanes 3 and 5 contain nucleosomes with H3(K56Q,C110A), with the top and bottom DNA strands 5' labeled with Cy3, respectively. (c and d) Denaturing polyacrylamide gel electrophoresis of the nucleosomal DNA cleaved by FeBABLE for 0 min, 5 min, and 10 min. Within each gel, lanes 1–3 and 10–12 contain sequencing tracks terminated with ddGTP, ddATP, and ddTTP, respectively; lanes 4–6 contain nucleosomes with H3(C110A)_{rec}; and lanes 7–9 contain nucleosomes with H3(K56Q,C110A). (c and d) Images of denaturing gels where the top and bottom DNA strands, respectively, are visualized by Cy3 fluorescence.

The change in the site exposure equilibrium of modified nucleosomes relative to unmodified nucleosomes is equal to the change in the probability that LexA can bind to its site, which extends 27 bp into the nucleosome. H3(K56ac,C110A) increases this value by 1.8 ± 0.4 times. The H3(K56Q) substitution, which has been used in numerous genetic studies as a mimic of H3(K56ac), increases the probability of LexA binding by 1.8 ± 0.4 and 1.9 ± 0.5 with and without H3(C110A), respectively. This demonstrates that the H3(C110A) mutation does not alter the influence of H3(K56Q) on nucleosomal DNA unwrapping, consistent with FRET efficiency measurements in the absence of LexA. H3(C110A)

does appear to modestly increase the absolute value of DNA site accessibility. However, by comparing H3(K56ac,C110A) and H3(K56Q,C110A) to H3(C110A)_{rec} and H3(C110A)_{syn}, we control for this effect.

Acetylation of H3(K56) facilitates protein binding by increasing the probability that the nucleosome is partially unwrapped

The increased protein accessibility induced by H3(K56ac) could result from changes in unwrapping, nucleosome DNA repositioning, or both. To resolve these possibilities, we determined the position of

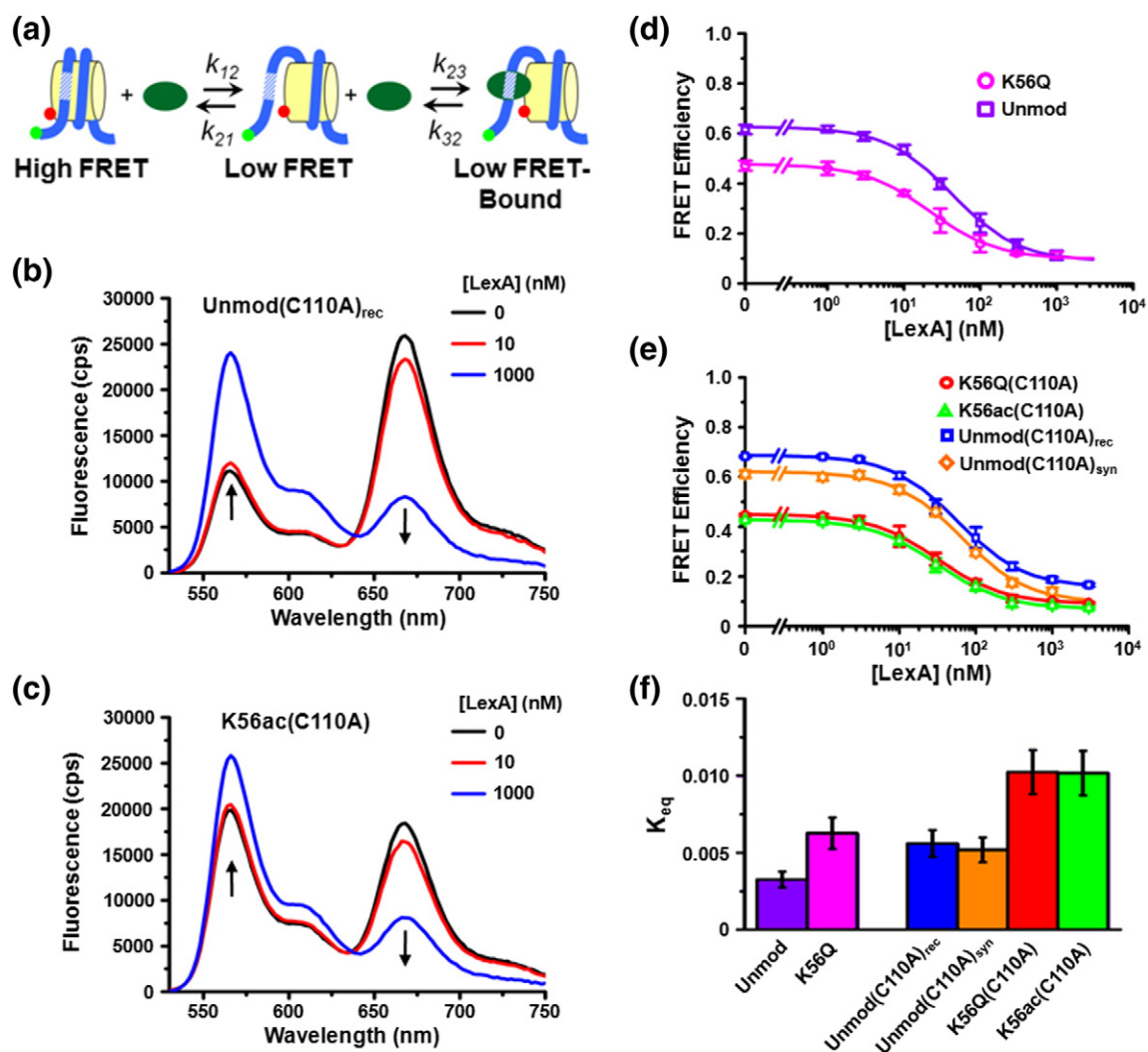


Fig. 8. H3(K56Q) and H3(K56ac) increase the site exposure equilibrium constant that facilitates LexA binding within nucleosomes at 1 mM Na⁺. (a) A three-state model for LexA binding to its target site within a nucleosome. (b and c) Fluorescence emission spectra at 0 nM (black), 10 nM (red), and 1000 nM (blue) LexA, with nucleosomes containing unmodified H3(C110A)_{rec} or H3(K56ac,C110A), respectively. The samples were excited at 510 nm (donor excitation). (d) Energy transfer efficiency determined by the (ratio)_A method *versus* the LexA concentration for nucleosomes containing unmodified H3 (purple) and H3(K56Q) (magenta). (e) The energy transfer efficiency determined by the (ratio)_A method *versus* the LexA concentration for nucleosomes containing unmodified H3, H3(C110A)_{rec} (blue), unmodified H3(C110A)_{syn} (orange), H3(K56Q,C110A) (red), and H3(K56ac,C110A) (green). Plots in (d) and (e) are the averages of three LexA titrations, and the error bars were determined from the standard deviation of the three measurements. The data were fitted to a noncooperative binding curve, which determines $S_{0.5-nuc}$ (the LexA concentration at which 50% of the nucleosomes are bound by LexA). (f) Equilibrium constants for site exposure for nucleosomes containing unmodified H3 (0.0033 ± 0.0005), H3(K56Q) (0.006 ± 0.001), unmodified H3(C110A)_{rec} (0.0055 ± 0.0009), unmodified H3(C110A)_{syn} (0.0052 ± 0.0008), H3(K56Q,C110A) (0.010 ± 0.002), and H3(K56ac) (0.010 ± 0.002). The equilibrium constants were determined from the ratio $K_{eq} = S_{0.5-DNA} / S_{0.5-nuc}$ (see [Materials and Methods](#) for details).

nucleosomes containing H3(C110A)_{rec} and H3(K56Q,C110A) in the presence of 1 μ M LexA by hydroxyl radical mapping. We found that nucleosomes in the presence of 1 μ M LexA retained a cleavage pattern identical to that of nucleosomes without LexA, as measured by denaturing PAGE (see Supplemental Information). LexA at this concentration of 1 μ M is bound to its target sequence

within nucleosomes, as measured by FRET efficiency (Fig. 8) and EMSA (Supplemental Information).

In addition, we carried out FRET efficiency studies with nucleosomes that were labeled at the 80th base pair with Cy3 (Fig. 9a). Based on the nucleosome crystal structure,⁴⁵ the distance between the Cy3 molecule and the nearest Cy5 molecule is about 2.3 nm, which converts to a FRET efficiency of 0.99;

we anticipate that this efficiency would be slightly reduced due to the 6-carbon linker used to attach Cy3 to the thymine base. If the LexA site were exposed only by repositioning, the distance between Cy3 and the nearest Cy5 would increase to 6.2 nm, which converts to a FRET efficiency of 0.45. We find that the FRET efficiency remains constant at 0.8 for nucleosomes containing unmodified H3, H3(K56Q), H3(C110A)_{recr}, H3(K56Q,C110A), and H3(K56ac,C110A) under conditions that are consistent with a full occupancy of the LexA binding site (Fig. 9).

The combination of FRET studies and hydroxyl radical mapping suggests that H3(K56Q) and H3(K56ac) do not increase DNA site accessibility via a nucleosome repositioning model. Instead, K56 acetylation and its mimic appear to increase LexA accessibility by increasing the probability that the nucleosome is partially unwrapped.

Acetylation of H3(K56) facilitates accessibility to DNA within nucleosomes at physiological ionic strength

Our initial studies were carried out at low ionic strength, but the physiologically relevant concentration of monovalent ions is 130–150 mM. Therefore, we carried out LexA binding studies with fluorophore-labeled nucleosomes at both 75 mM and 130 mM NaCl, as described above for 1 mM Na⁺. We determined the $S_{0.5-nuc}$ values for H3(C110A)_{recr}, H3(C110A)_{synr}, H3(K56Q,C110A), and H3(K56ac,C110A) at 75 mM and 130 mM NaCl (Fig. 10a and b, Table 2). We were unable to determine the $S_{0.5-DNA}$ value by EMSA because of the increase in NaCl. Therefore, we determined the K_{eq} values for H3(K56Q,C110A) and H3(K56ac,C110A) nucleosomes relative to unmodified nucleosomes. At 75 mM, $K_{eq-H3(K56ac)}/K_{eq-Unmod} = 3.3 \pm 0.4$ and $K_{eq-H3(K56Q)}/K_{eq-Unmod} = 2.5 \pm 0.3$, while at 130 mM, $K_{eq-H3(K56ac)}/K_{eq-Unmod} = 3.3 \pm 0.4$ and $K_{eq-H3(K56Q)}/K_{eq-Unmod} = 2.5 \pm 0.3$ (Fig. 10c, Table 2).

These results imply that at the physiological ionic strength of 130 mM, H3(K56ac) increases DNA unwrapping fluctuations that expose the LexA target site 3-fold, in turn resulting in a 3-fold increase in LexA binding to its target site. Furthermore, we find that H3(K56Q) increases DNA site exposure similarly to H3(K56ac) at physiological ionic strength, suggesting that H3(K56Q) is a good acetylation mimic of H3(K56ac) for *in vivo* studies.

Discussion

PTMs of histones occur throughout the protein sequence with multiple disparate types of modification often detected on a single histone.^{9,51} Current methods of preparing modified histones are limited to the site-specific introduction of a

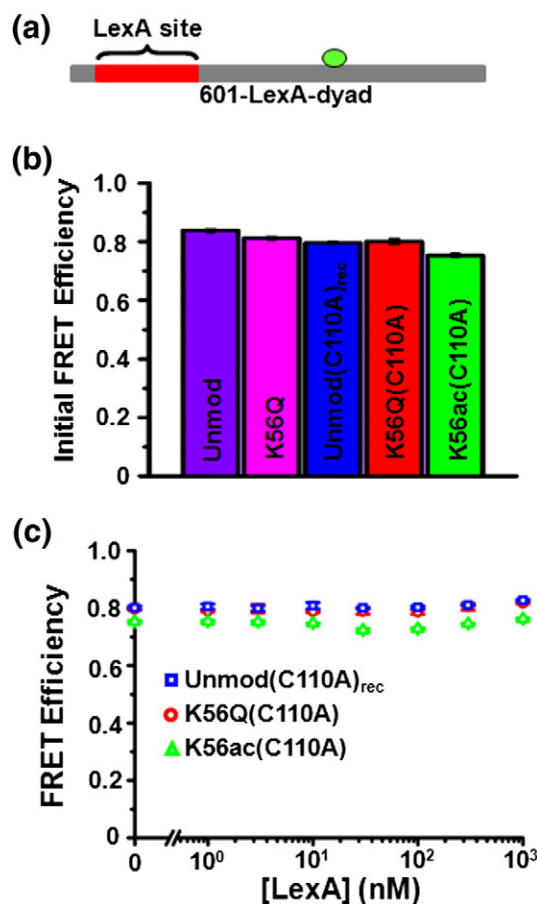


Fig. 9. (a) The 147-bp DNA molecule 601-LexA-dyad contains the 601 positioning sequence with the LexA binding site at base pairs 8–27 and with a Cy3 fluorophore attached to the 80th base pair of the DNA molecule. (b) The FRET efficiency, as determined by the (ratio)_A method, of nucleosomes containing unmodified H3, H3(K56Q), H3(C110A)_{recr}, H3(K56Q,C110A), and H3(K56ac,C110A). Each nucleosome contained the 601-LexA-dyad DNA molecule. The error bars were determined from the standard deviation of three separate measurements. (c) The energy transfer efficiency determined by the (ratio)_A method versus the LexA concentration for H3(C110A)_{recr}, H3(K56Q,C110A), and H3(K56ac,C110A) nucleosomes containing the 601-dyad DNA construct (Fig. 3a). Each plot is the average of at least three LexA titrations, and the error bars were determined from the standard deviation of the three measurements.

single type of modification within a histone protein^{15,20,21} or a variety of modifications within a localized region of the histone protein.^{12,14,16–18,52}

We have established a method for incorporating one or several PTMs into a histone protein by sequential NCL, targeting the common Ala residue as a ligation junction. The procedure thus generates a native-like histone containing only the PTM(s) of interest with no nonnative residues other than the well-studied C110A. In other studies, the

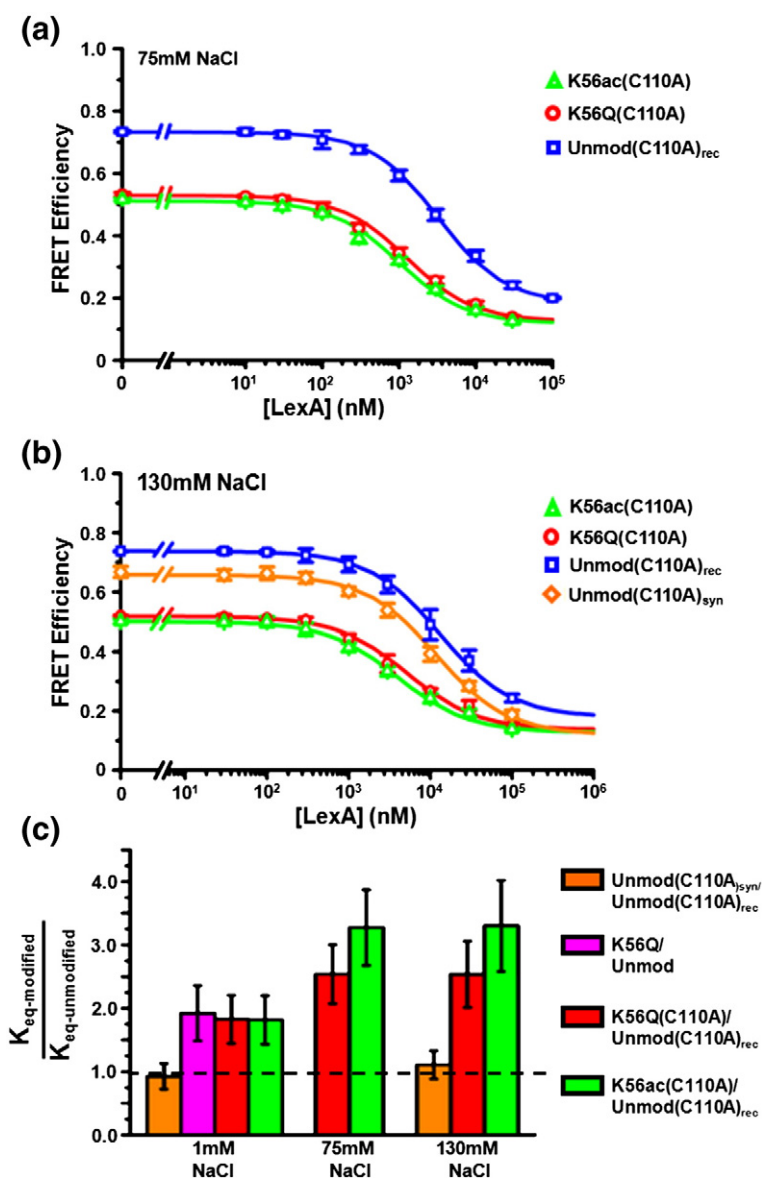


Fig. 10. H3(K56ac) and H3(K56Q) enhance LexA binding to its DNA target sequence within nucleosomes at physiological ionic strength. (a and b) Energy transfer efficiency in the presence of 75 mM and 130 mM NaCl, respectively, as determined by the (ratio)_A method versus the LexA concentration for nucleosomes containing unmodified H3(C110A)_{rec} (blue), unmodified H3(C110A)_{syn} (orange), H3(K56Q, C110A) (red), and H3(K56ac, C110A) (green). Plots in (a) and (b) are the average of three LexA titrations, and the error bars were determined from the standard deviation of the three measurements. The data were fitted to a noncooperative binding curve, which determines $S_{0.5-nuc}$ (the LexA concentration at which 50% of the nucleosomes are bound by LexA). (c) Equilibrium constants: at 1 mM Na⁺, H3(C110A)_{syn} relative to H3(C110A)_{rec} (0.93 ± 0.20), H3(K56Q) relative to H3(C110A)_{rec} (1.9 ± 0.4), H3(K56Q, C110A) relative to H3(C110A)_{rec} (1.8 ± 0.4); at 75 mM NaCl, H3(K56Q, C110A) relative to H3(C110A)_{rec} (2.5 ± 0.3), and H3(K56ac, C110A) relative to H3(C110A)_{rec} (3.3 ± 0.4); at 130 mM NaCl, H3(C110A)_{syn} relative to H3(C110A)_{rec} (1.11 ± 0.22), H3(K56Q, C110A) relative to H3(C110A)_{rec} (2.5 ± 0.3), and H3(K56ac, C110A) relative to H3(C110A)_{rec} (3.3 ± 0.4).

introduction of select nonnative Cys residues through ligation in the unstructured nucleosome tail has had a negligible effect on nucleosome dynamics.^{12,16,52} Similarly, desulfurization has been coupled with ligation in the context of introducing modifications into the N-terminal and C-terminal tails of semisynthetic histones.^{17–19} Our work demonstrates that the semiconservative introduction of Cys residues into the nucleosome core can perturb DNA wrapping. In the context of synthetic histones, this effect can be mitigated by conversion into a native Ala residue. However, the impact of these substitutions must be considered when interpreting biochemical or biophysical measurements that require the introduction of nonnative Cys sites throughout the nucleosome.

Although our initial study was restricted to the synthesis and characterization of unmodified H3 and H3(K56ac), this method is limited only by the synthesis of individual peptide segments and would allow for the introduction of PTMs throughout histone H3. As H3 is the largest of the core histone proteins, our success suggests that the total synthesis strategy may be applied to all of the histone proteins, including rare variants. These methods should therefore be useful in determining the function and biophysical properties associated with the voluminous numbers of cellular PTMs.

Using sequential NCL methodology, we have engineered and characterized nucleosomes containing K56ac within histone H3. Our measurements of nucleosomes containing K56ac are in agreement with

the results of Neumann *et al.*, which show that K56ac increases the population of nucleosomes that are partially unwrapped at the DNA entry–exit region by up to seven times at low ionic strength. We extend these studies to demonstrate that DNA unwrapping in the DNA entry–exit region facilitates protein binding 27 bp into the nucleosome by a factor of 1.8 under low ionic conditions ($0.5\times$ TE buffer).¹⁵ In addition, we determined the influence of K56ac on DNA unwrapping and protein binding within the nucleosome at physiological ionic strength (130 mM NaCl). We find that this enhances the influence of K56ac on DNA unwrapping such that protein binding is increased 3.3 times to 27 bp into the nucleosome. These studies are consistent with enhanced accessibility to transcription factors and DNA repair components in chromatin regions containing K56ac within histone H3.

Interestingly, Neumann *et al.* found that the FRET distribution was not altered 27 bp into the nucleosomes with K56ac. This appears to be in contrast to our result that K56ac facilitates protein binding to a site that extends 27 bp into the nucleosome. We can understand this apparent discrepancy by considering the previously reported cooperativity of adjacent DNA target sites within a nucleosome.^{5,6} Protein binding to the outer DNA target site within the nucleosome facilitates binding to the inner target site. In our case, K56ac appears to act as the outer adjacent site that facilitates LexA binding to its target site within the nucleosome.

The acetylation of H3(K56) has also been shown to be important for transcriptional regulation.^{30,34,35,53} For example, K56ac within H3 has been implicated in the transcriptional regulation of the *HTA1* and *SUC2* genes.³⁰ Interestingly, studies carried out using ChiP have demonstrated that the occupancy of the SWI/SNF chromatin remodeler Snf5 is reduced 2-fold to 3-fold by the H3(K56R) substitution that mimics unacetylated lysine in the promoter region and the coding region of the *HTA1* and *SUC2* genes.³⁰ Such a reduction in Snf5 occupancy could be explained by the 3-fold reduction that we observe in site accessibility when nucleosomes are not acetylated at H3(K56). However, it is also possible that these changes in occupancy result from indirect effects of acetylation, since SWI/SNF is known to contact the nucleosome core particle over a large surface area rather than through a specific interaction with H3(K56).⁵⁴ For example, we find that acetylation loosens nucleosomal DNA in the entry–exit region, which could influence the formaldehyde cross-linking required to detect SWI/SNF binding in this study.

Our quantitative measurements of LexA protein accessibility by K56ac and K56Q are in agreement with multiple studies. During DNA replication, nucleosomes are assembled with H3(K56ac).³⁰ Polymerase misincorporation errors and DNA lesions result in mismatched nucleotides, replication

fork collapse, and DNA double-strand breaks that must be repaired to ensure genomic stability.⁵⁵ Deletion of *rtt109*, which acetylates H3(K56), or mutation of H3(K56) to Arg [H3(K56R)], which mimics unacetylated H3, causes large defects in postreplication DNA repair³² and leads to genomic instability.³³ Recently, we have shown that the DNA mismatch recognition complex hMSH2–hMSH6 can remodel nucleosomes near a mismatch, and that this activity is enhanced 2-fold for nucleosomes containing H3(K56Q).⁵⁶ This result is consistent with our observation that H3(K56Q)-containing nucleosomes increase DNA accessibility by a factor of 3 at physiological ionic strength. Together, these observations suggest that increased DNA site accessibility near the DNA entry–exit region associated with H3(K56ac) facilitates nucleosome remodeling by hMSH2–hMSH6.

Numerous studies, including a number of genetic studies that found phenotypes in both gene expression and DNA repair, use H3(K56Q) substitution to mimic lysine acetylation.^{31,35} Our study suggests that similar phenotypes will result in cells that are constitutively acetylated at H3(K56). Recently, the crystal structure of nucleosomes containing H3(K56Q) was reported by Watanabe *et al.*³⁶ They found that K56Q did not impact the structure of the fully wrapped state of the nucleosome, consistent with a role for K56 acetylation in nucleosome dynamics. They also reported that H3(K56Q) did not influence the compaction of nucleosome arrays, regardless of nucleosome density. However, H3(K56Q) dramatically reduced interactions between multiple arrays of nucleosomes; thus, H3(K56ac) may function to reduce chromatin–chromatin interactions to help keep nucleosome-free regions accessible for DNA replication and repair. Their studies relied on the assumption that H3(K56Q) accurately mimics H3(K56ac). Our studies, which demonstrate that H3(K56Q) mimics H3(K56ac), indicate that this assumption is correct.

In conclusion, our studies demonstrate the power of sequential NCL to engineer fully synthetic histones with precise PTMs that can be combined with quantitative biophysical methodologies to determine the function of these PTMs in the context of nucleosomes. Ongoing studies will test the function of multiple PTMs found in biologically relevant processes.

Materials and Methods

Peptide synthesis

Peptides (Table 1) were synthesized manually using standard Boc-N- α protection strategies and *in situ* neutralization protocols⁵⁷ utilizing 1-*H*-benzotriazolium

activation. C-terminal peptides C1 and C2 were synthesized on preloaded Boc-Ala-PAM resin (Novabiochem). Thioester peptides N1, N2, M1, and M2 were synthesized on 4-methylbenzhydrylamine resin with a mercaptopropionamide linker to generate the C-terminal thioester moiety necessary for subsequent ligation.⁵⁸ Acetylated lysine was incorporated as the commercially available Boc-protected derivative *N*- α -t-Boc-acetyl-lysine (Novabiochem), and the protected N-terminal Cys was incorporated as thiaproline (Boc-L-thiazolidine-4-carboxylic acid; Bachem). Peptides were cleaved from solid support under standard anhydrous hydrogen fluoride cleavage conditions utilizing *p*-cresol as scavenger. Following synthesis and purification, all peptide purities were assessed by RP-HPLC as >95%, with the exception of peptide M1, which contained a mixture of Met and Met(O) species.

Synthesis of H3(R40C,K56ac,S96C,C110A)

Synthetic H3(R40C,K56ac,S96C,C110A) proteins were generated by sequential NCL (Fig. 1a). In the first step of the ligation, peptide M1 propionamide thioester was resuspended with a 5-fold to 10-fold molar excess of peptide C1 in 100 mM Hepes (pH 7.5), 1 M NaCl, 50 mM sodium mercaptoethanesulfonate (MesNa), and 6 M guanidinium hydrochloride (GdnHCl), and reacted for 2 days at 25 °C. Upon completion, direct addition of 500 mM methoxylamine HCl to the ligation mixture generated the free N-terminal Cys by unmasking Thz.²⁴ Complete conversion into the desired terminal Cys was observed within 6 h. The M1C1 product was purified to >95% by RP-HPLC with a gradient of 22.5–50% isopropanol/0.1% trifluoroacetic acid (TFA) with a C4 Vydac column at 45 °C (Fig. 2a), and the product identity was confirmed by MALDI-TOF MS.

Purified ligation product M1C1 was resuspended with a 20-fold molar excess of peptide N1 in 100 mM Hepes (pH 7.5), 1 M NaCl, 50 mM MesNa, 10 mM tris(2-carboxyethyl)phosphine (TCEP), and 6 M GdnHCl. The ligation mixture was nutated for 24 h at 25 °C to generate the site-specifically modified H3(R40C,K56ac,S96C,C110A). The final product was purified by RP-HPLC with a step gradient of acetonitrile/0.1% TFA on a Supelco Widebore C18 column at 25 °C, as follows: 11–16% over 5 min, 16–43% over 5 min, and 43–66% over 30 min. Fractions identified by MALDI-TOF MS to contain full-length H3(R40C,K56ac,S96C) with and without the Met(O) species were pooled and lyophilized.

Reduction of Met(O) to Met in H3(R40C,K56ac,S96C,C110A) was accomplished by suspending the lyophilized protein in 200 μ l of TFA with 25 μ l of dimethylsulfide and 0.045 M sodium iodide.⁵⁹ Reduction was allowed to proceed for 1 h on ice until complete, as monitored by MALDI-TOF MS (Fig. 2c). Reduced protein was precipitated and washed with cold anhydrous diethyl ether, then purified by RP-HPLC on a Supelco Widebore C18 column with a gradient of 43–66% acetonitrile/0.1% TFA (Fig. 2d). MALDI-TOF MS confirmed that the Met(O) species was absent in the collected fraction. The total synthesis of H3(R40C,K56ac,S96C,C110A), as described previously, provided an overall ligation yield of 2% (measured by UV quantification).

Synthesis of H3(A47C,K56ac,A91C,C110A)

Sequential NCL was employed to generate synthetic H3(A47C,K56ac,A91C,C110A) (Fig. 1). Thioester peptide M2 (typically 0.5 mg) was resuspended with a 2.5-fold molar excess of C2 in 100 mM phosphate (pH 7.5), 1 M NaCl, 60 mM 4-mercaptophenylacetic acid (MPAA), 20 mM TCEP, and 50% trifluoroethanol, and reacted for 48 h at 25 °C (Fig. 5a). We determined that when ring opening was carried out prior to the first purification step, we observed a backformation of Thz-M2C2 over the course of the second ligation reaction. We attribute this to a copurification of trace amounts of formaldehyde generated in the cleavage of a His(Bom) side-chain-protecting group in peptide N2. This back-ring closure was minimized by the presence of methoxylamine in the ligation reaction. We therefore purified Thz-M2C2 prior to the ring-opening step. While the ligation product partially precipitated under these buffer conditions, reaction in a phosphate/guanidinium buffer prevented this problem and was used in future ligation iterations. The product was resuspended in 100 mM phosphate (pH 7.5), 1 M NaCl, and 6 M GdnHCl with 60 mM TCEP, and purified by RP-HPLC on a Supelco Widebore C18 column with a gradient of 32–59% acetonitrile/0.1% TFA.

Lyophilized ligation product Thz-M2C2 was resuspended with 100 mM phosphate (pH 7.5), 1 M NaCl, 6 M GdnHCl, and 20 mM TCEP. Methoxylamine hydrochloride (350 mM) was added to convert the N-terminal Thz into Cys. Deprotection was allowed to proceed for 6 h at 25 °C (Fig. 5b). The mixture was adjusted to pH 7.5 with NaOH, and then MesNa was added to the mixture to a final concentration of 100 mM. The ligation was initiated with the addition of a 5-fold molar excess of peptide N2. Ligations were monitored by RP-HPLC and SDS-PAGE for 4–6 days at 25 °C until no additional product formation was observed (Fig. 5c). We attribute the slow product formation to the C-terminal residue of peptide N2 (Val), which is known to result in slow ligation.⁶⁰ The crude ligation mixture was carried forward for desulfurization to reveal the final H3(K56ac,C110A) protein.

Desulfurization of H3(A47C,K56ac,A91C,C110A) (N2M2C2) to yield H3(K56ac,C110A)

The H3(A47C,K56ac,A91C,C110A) ligation mixture was directly desulfurized prior to purification under free-radical desulfurization conditions.⁴⁷ The mixture was adjusted to final concentrations of 50 mM phosphate (pH 7.5), 500 mM NaCl, 0.3 M TCEP, 100 mM MesNa, and 5 M GdnHCl, and the sample was sparged with argon for 30 min. Desulfurization was initiated with the addition of VA-044US (Wako Chemical) to a final concentration of 10 mM at 42 °C, and the reaction was allowed to proceed until complete, as monitored by MALDI-TOF MS analysis (minimum of 3 h; Fig. 5d). The final desulfurized product H3(K56ac,C110A) was purified by RP-HPLC with a gradient of 41–59% acetonitrile/0.1% TFA on a Supelco Widebore C18 column (Fig. 5e). A typical ligation began with 0.5 mg of limiting peptide M2. The ligation and desulfurization procedures described yielded 93 μ g of the final product H3(K56ac,C110A), as determined by UV

quantification on a NanoDrop 1000 (Thermo Scientific), for an overall synthetic yield of 7%. We attribute this increase in synthetic yield to the use of only two chromatography steps through our ligation pathway: purification of Thz-M2C2 and purification of the final desulfurized product H3(K56ac,C110A). If Met(O) species was observed in the full-length native H3-K56ac, reduction was carried out on the purified product without the need for further purification.

Total synthesis of H3(C110A)

Peptide M3, the unmodified variant of peptide M2, was synthesized and used for the total synthesis of H3(C110A)_{syn} under the preceding conditions, with the following changes. Following Thz deprotection of the purified ligation product Thz-M3C2, the pH was adjusted to 7.5, and the ligation was initiated by addition of 75 mM MPAA and a 20-fold molar excess of peptide N2. The ligation progress was monitored for 3 days, and the resulting reaction mixture was dialyzed to remove MPAA prior to desulfurization, as described previously. The fully synthetic H3(C110A)_{syn} was purified by RP-HPLC to yield 120 µg, as determined by UV quantitation, and the protein identity was confirmed by MALDI-TOF MS (Fig. 5f).

Preparation of DNA constructs

The DNA molecules 601-end, 601-LexA-end (Fig. 3a), and 601-LexA-dyad (Fig. 10a) were prepared by PCR with Cy3-labeled oligonucleotides from a plasmid containing the 601 positioning sequence with or without a LexA binding site at bases 8–27.³ Oligonucleotides were labeled with a Cy3 NHS ester (GE Healthcare) at an amino group attached to the 5' end or to a modified internal thymine and then purified by reverse-phase liquid chromatography on a C18 Vydac column. The oligonucleotides used for amplification are as follows: 601-LexA-end, Cy3-CTGGA-GATACTGTATGAGCATACAGTACAATTGGTC and ACAGGATGTATATATCTGACACGTGCCTGGAGACTA; 601-LexA-dyad, CTGGAGATACTGTATGAGCATACAG-TACAATTGGTCGTAGCA and ACAGGATGTATA-TATCTGACACGTGCCTGGAGACTAGGGAG-TAATCCCCTGGCGTTAAACGCGG(T-Cy3)GGACA; 601-end, Cy3-CTGGAGAATCCCGGTGCCG and TCAG-GATGTATATATCTGACACGTGCCTGGAGACTA. Following PCR amplification, each DNA molecule was purified by HPLC with a Gen-Pak Fax column (Waters).

Preparation of HOs and LexA protein

Recombinant histones were expressed and purified as previously described.⁶¹ Plasmids encoding histones H2A (K119C), H2B, H3, and H4 were generous gifts from Dr. Karolin Luger (Colorado State University) and Dr. Jonathan Widom (Northwestern University). Mutations H3(R40C), H3(S96C), H3(C110A), H3(K56Q), and H4 (S47C) were introduced by site-directed mutagenesis (Stratagene). H2A(K119C) was labeled before or after HO refolding with Cy5 maleamide (GE Healthcare). We achieved a labeling efficiency of 75–90%, as determined by

mass spectrometry and UV absorption. Histones H2A (K119C), H2B, and H4, and either H3, H3(C110A)_{rec}, H3(C110A)_{syn}, H3(K56Q), H3(K56Q,C110A), or H3(K56ac, C110A) were combined at equal molar ratios and refolded as previously described.³ The purity of each octamer was confirmed by SDS-PAGE and mass spectrometry. LexA protein was expressed and purified from the pJWL288 plasmid (gift from Dr. Jonathan Widom) as previously described.⁶²

H2A histone labeling

H2A was labeled with Cy5 before octamer refolding for octamers that contained H3(C110), while H2A was labeled either before or after refolding for octamers that contained H3(C110A). We found that the labeling method did not influence our FRET measurements. H2A was labeled before octamer refolding by first resuspending H2A (K119C) to 1.2 mg/ml in 1.5 M GdnHCl and 800 mM Hepes (pH 7.1) and by purging under argon atmosphere with stirring for 1 h at 25 °C. TCEP (pH 7.1) was added to a final concentration of 0.7 mM and incubated for 20 min at 25 °C with stirring under argon. Cy5 maleamide (GE Healthcare) was resuspended to 7 mg/ml in anhydrous dimethylformamide and added dropwise with stirring to a final concentration of 1.1 mg/ml. The reaction was allowed to proceed for 5 h at 25 °C with stirring under argon before being quenched with 10 mM DTT. Unreacted dye was removed from conjugated protein on a Sephadex G-25 column (Amersham) at 1 ml/min equilibrated with TU1000 buffer [6 M urea, 1 M NaCl, 10 mM Tris (pH 9), and 1 mM β-mercaptoethanol]. Purified fractions were dialyzed extensively against 2 mM β-mercaptoethanol before lyophilization.

H2A was Cy5 labeled following octamer refolding by resuspending purified HO containing H2A(K119C) to 1 mg/ml in 2 M NaCl, 200 mM Hepes (pH 7.1), and 1 mM EDTA, and then by purging under argon atmosphere without stirring for 1 h at 4 °C. TCEP (pH 7.1) was added to a final concentration of 0.7 mM and incubated under argon atmosphere for 20 min at 4 °C. Cy5 maleamide (GE Healthcare) was resuspended to 2.5 mg/ml in anhydrous dimethylformamide and added dropwise with thorough mixing to a final concentration of 0.35 mg/ml. The reaction was allowed to proceed for 2 h at 25 °C on a shaker rotisserie and then transferred to 4 °C overnight before being quenched with 10 mM DTT. Unreacted dye was removed by sucrose gradient purification of reconstituted nucleosome (see the text below).

Nucleosome preparation

Nucleosomes were reconstituted by salt double dialysis⁶³ with 7 µg of DNA and 5 µg of HO. DNA and HO were mixed in 50 µl of 0.5× TE buffer (10 mM Tris, 1 mM EDTA, pH 8.0), 2 M NaCl, and 1 mM benzamidine (BZA). The sample was loaded into an engineered 50-µl dialysis chamber, which was placed in a large dialysis tube with 80 ml of 0.5× TE buffer (pH 8.0), 2 M NaCl, and 1 mM BZA. The large tube was extensively dialyzed against 0.5× TE buffer (pH 8.0) with 1 mM BZA. The 50-µl sample was extracted from the dialysis button and purified by sucrose gradient centrifugation (Fig. 3d).

Mapping nucleosome positions with hydroxyl radical cleavage

Nucleosome positions were mapped using FeBABE protein cutting reagent (Thermo Scientific) conjugated to H4(S47C). Histones H2A, H2B, and H4(S47C), and either H3(C110A)_{rec} or H3(K56Q,C110A) were combined at equal molar ratios and refolded as previously described.³ HO was extensively dialyzed against “labeling buffer” [2 M NaCl, 30 mM Hepes (pH 8.2), 5% glycerol, and 4 mM EDTA]. For FeBABE conjugation, HO was resuspended to 1 mg/mL in labeling buffer and purged under argon atmosphere without stirring for 1 h at 4 °C. FeBABE was resuspended to 5 mg/ml in degassed labeling buffer and added dropwise to HO with thorough mixing to a final concentration of 0.8 mg/ml. The reaction was allowed to proceed for 2 h at 25 °C on a shaker rotisserie and then extensively dialyzed against 2 M NaCl, 50 mM Tris (pH 8.2), 50% glycerol, and 0.1 mM EDTA at 4 °C to removed unconjugated FeBABE.

Nucleosomes containing 601-LexA with Cy3 on the 5' end of the forward or reverse strand were reconstituted by salt double dialysis⁶³ as previously described (Fig. 7b). To perform hydroxyl radical mapping, we resuspended nucleosomes to 25 nM on ice in degassed 20 mM Tris (pH 7.5), 0.1 mM EDTA, and 10% glycerol. Then 40 mM L-ascorbic acid in degassed 20 mM Tris (pH 7.5), 10 mM EDTA, and 80 mM hydrogen peroxide in degassed 20 mM Tris (pH 7.5) and 10 mM EDTA were added in quick succession to the nucleosomes with thorough mixing to final concentrations of 4 mM and 8 mM, respectively. The reaction was allowed to proceed for 10 min and 20 min before 7 µl of the reaction mixture was transferred to 3 µl of 1.3 M Tris (pH 7.5). Samples were mixed with an equal volume of formamide and resolved by 12% denaturing PAGE in 7 M urea and 1× Tris-borate-EDTA. The sequence markers were prepared with a SequiTherm Excel II DNA sequencing kit (Epicenter) using Cy3-labeled primers, a 601-LexA DNA template, and either ddGTP, ddATP, or ddTTP. Results were imaged by a Typhoon 8600 variable mode imager (GE Healthcare) (Fig. 7).

FRET efficiency measurements

FRET efficiency measurements were determined by the (ratio)_A method as previously described.⁴⁶ The fluorescence emission spectra were measured at 25 °C with a Fluoromax-3 (Horiba) photon-counting steady-state fluorometer. Cy3/Cy5-labeled nucleosomes (5 nM) were excited at 510 nm and 610 nm, while the emission spectra were collected from 530 nm to 750 nm and from 630 nm to 750 nm, respectively. The FRET efficiencies E were measured from acceptor emission using the (ratio)_A equation: $E = 2[(\epsilon^A(v'')F^A(v')/F^A(v'') - \epsilon^A(v'))]/[(\epsilon^D(v')d^+]$, where $v' = 510$ nm for donor (D) excitation and $v'' = 610$ nm for direct acceptor (A) excitation. A prefactor of 2 reflects the presence of two acceptor molecules per donor molecule. $F^A(v')$ is the fluorescence emission of A after the subtraction of overlapping D emission when excited at 510 nm. $F^A(v'')$ is the fluorescence emission of A when excited at 610 nm. $\epsilon^D(v')$, $\epsilon^A(v')$, and $\epsilon^A(v'')$ are the molar extinction coefficients of D and A at v' and v'' . d^+ is the fractional labeling of D, which is 1.

Site accessibility equilibrium measurements

The equilibrium constants for site accessibility were determined from the reduction in FRET efficiency as LexA binds to its target site buried within the nucleosome (Figs. 4 and 8).³ LexA was titrated from 0 µM to 3 µM with 5 nM Cy3/Cy5-labeled nucleosomes in 0.5× TE buffer. The FRET efficiency was determined by the (ratio)_A method, performed in triplicate, for each LexA concentration. The average FRET efficiency *versus* the LexA concentration was fitted to a noncooperative binding isotherm: $E = E_F + (E_0 - E_F)/(1 + [\text{LexA}]/S_{0.5})$, where E is the FRET efficiency, E_0 is the FRET efficiency without LexA, E_F is the FRET efficiency at high LexA concentration, and $S_{0.5-nuc}$ is the LexA concentration at which the FRET efficiency has been reduced by half [i.e., $E = (E_0 + E_F)/2$]. The equilibrium constant K_{eq} was determined from $K_{eq} = S_{0.5-DNA}/S_{0.5-nuc}$, which is true for the three-state model (Fig. 8a) when $S_{0.5-DNA} \ll S_{0.5-nuc}$, as is the case here. $S_{0.5-DNA}$ is the LexA concentration at which its target site within naked DNA is 50% bound by LexA and was determined by gel shift on a polyacrylamide gel (see Supplemental Information).

Supplementary materials related to this article can be found online at [doi:10.1016/j.jmb.2011.01.003](https://doi.org/10.1016/j.jmb.2011.01.003)

Acknowledgements

We thank Richard Fishel for extensive discussions and careful editing of the manuscript. We thank Jonathan Widom and Karolin Luger for the *X. laevis* histone and LexA expression vectors. We are grateful to Dongping Zhong for access to Fluoromax-3, to Karin Musier-Forsyth for access to a Typhoon Trio fluorescence scanner and a fluorescence plate reader, and to Ross Dalbey for access to a table-top ultracentrifuge. We gratefully acknowledge support from the American Heart Association (predoctoral fellowship 0815460D to J.A.N.), the National Institutes of Health (grant GM083055 to M.G.P. and J.J.O.), the National Science Foundation (career grant MCB0845696 to J.J.O.), and the Burroughs Wellcome Fund (CAREER Award in the Basic Biomedical Sciences to M.G.P.).

References

1. Van Holde, K. E. (1989). *Chromatin*. Springer-Verlag, New York, NY.
2. Polach, K. J. & Widom, J. (1995). Mechanism of protein access to specific DNA sequences in chromatin: a dynamic equilibrium model for gene regulation. *J. Mol. Biol.* **254**, 130–149.
3. Li, G. & Widom, J. (2004). Nucleosomes facilitate their own invasion. *Nat. Struct. Mol. Biol.* **11**, 763–769.
4. Bucceri, A., Kapitzka, K. & Thoma, F. (2006). Rapid accessibility of nucleosomal DNA in yeast on a second time scale. *EMBO J.* **25**, 3123–3132.

5. Adams, C. C. & Workman, J. L. (1995). Binding of disparate transcriptional activators to nucleosomal DNA is inherently cooperative. *Mol. Cell. Biol.* **15**, 1405–1421.
6. Polach, K. J. & Widom, J. (1996). A model for the cooperative binding of eukaryotic regulatory proteins to nucleosomal target sites. *J. Mol. Biol.* **258**, 800–812.
7. Bernstein, B. E., Liu, C. L., Humphrey, E. L., Perlstein, E. O. & Schreiber, S. L. (2004). Global nucleosome occupancy in yeast. *Genome Biol.* **5**, R62.
8. Tirosh, I. & Barkai, N. (2008). Two strategies for gene regulation by promoter nucleosomes. *Genome Res.* **18**, 1084–1091.
9. Su, X., Zhang, L., Lucas, D. M., Davis, M. E., Knapp, A. R., Green-Church, K. B. *et al.* (2007). Histone H4 acetylation dynamics determined by stable isotope labeling with amino acids in cell culture and mass spectrometry. *Anal. Biochem.* **363**, 22–34.
10. Fischle, W., Wang, Y. & Allis, C. D. (2003). Histone and chromatin cross-talk. *Curr. Opin. Cell Biol.* **15**, 172–183.
11. Taverna, S. D., Li, H., Ruthenburg, A. J., Allis, C. D. & Patel, D. J. (2007). How chromatin-binding modules interpret histone modifications: lessons from professional pocket pickers. *Nat. Struct. Mol. Biol.* **14**, 1025–1040.
12. Shogren-Knaak, M., Ishii, H., Sun, J. M., Pazin, M. J., Davie, J. R. & Peterson, C. L. (2006). Histone H4-K16 acetylation controls chromatin structure and protein interactions. *Science*, **311**, 844–847.
13. Cosgrove, M. S., Boeke, J. D. & Wolberger, C. (2004). Regulated nucleosome mobility and the histone code. *Nat. Struct. Mol. Biol.* **11**, 1037–1043.
14. Manohar, M., Mooney, A. M., North, J. A., Nakkula, R. J., Picking, J. W., Edon, A. *et al.* (2009). Acetylation of histone H3 at the nucleosome dyad alters DNA–histone binding. *J. Biol. Chem.* **284**, 23312–23321.
15. Neumann, H., Hancock, S. M., Buning, R., Routh, A., Chapman, L., Somers, J. *et al.* (2009). A method for genetically installing site-specific acetylation in recombinant histones defines the effects of H3 K56 acetylation. *Mol. Cell.* **36**, 153–163.
16. Shogren-Knaak, M. A., Fry, C. J. & Peterson, C. L. (2003). A native peptide ligation strategy for deciphering nucleosomal histone modifications. *J. Biol. Chem.* **278**, 15744–15748.
17. He, S., Bauman, D., Davis, J. S., Loyola, A., Nishioka, K., Gronlund, J. L. *et al.* (2003). Facile synthesis of site-specifically acetylated and methylated histone proteins: reagents for evaluation of the histone code hypothesis. *Proc. Natl Acad. Sci. USA*, **100**, 12033–12038.
18. McGinty, R. K., Kim, J., Chatterjee, C., Roeder, R. G. & Muir, T. W. (2008). Chemically ubiquitylated histone H2B stimulates hDot1L-mediated intranucleosomal methylation. *Nature*, **453**, 812–816.
19. Chiang, K. P., Jensen, M. S., McGinty, R. K. & Muir, T. W. (2009). A semisynthetic strategy to generate phosphorylated and acetylated histone H2B. *Chem-BioChem*, **10**, 2182–2187.
20. Simon, M. D., Chu, F., Racki, L. R., de la Cruz, C. C., Burlingame, A. L., Panning, B. *et al.* (2007). The site-specific installation of methyl-lysine analogs into recombinant histones. *Cell*, **128**, 1003–1012.
21. Guo, J., Wang, J., Lee, J. S. & Schultz, P. G. (2008). Site-specific incorporation of methyl- and acetyl-lysine analogues into recombinant proteins. *Angew. Chem. Int. Ed. Engl.* **47**, 6399–6401.
22. Nguyen, D. P., Alai, M. M., Kapadnis, P. B., Neumann, H. & Chin, J. W. (2009). Genetically encoding *N*(epsilon)-methyl-L-lysine in recombinant histones. *J. Am. Chem. Soc.* **131**, 14194–14195.
23. Lennartsson, A. & Ekwall, K. (2009). Histone modification patterns and epigenetic codes. *Biochim. Biophys. Acta*, **1790**, 863–868.
24. Bang, D. & Kent, S. B. (2004). A one-pot total synthesis of crambin. *Angew. Chem. Int. Ed. Engl.* **43**, 2534–2538.
25. Kent, S. B. (2009). Total chemical synthesis of proteins. *Chem. Soc. Rev.* **38**, 338–351.
26. Ottesen, J. J., Bar-Dagan, M., Giovani, B. & Muir, T. W. (2008). An amalgamation of solid phase peptide synthesis and ribosomal peptide synthesis. *Biopolymers*, **90**, 406–414.
27. Yamamoto, N., Tanabe, Y., Okamoto, R., Dawson, P. E. & Kajihara, Y. (2008). Chemical synthesis of a glycoprotein having an intact human complex-type sialyloligosaccharide under the Boc and Fmoc synthetic strategies. *J. Am. Chem. Soc.* **130**, 501–510.
28. Downs, J. A. (2008). Histone H3 K56 acetylation, chromatin assembly, and the DNA damage checkpoint. *DNA Repair (Amsterdam)*, **7**, 2020–2024.
29. Ozdemir, A., Masumoto, H., Fitzjohn, P., Verreault, A. & Logie, C. (2006). Histone H3 lysine 56 acetylation: a new twist in the chromosome cycle. *Cell Cycle*, **5**, 2602–2608.
30. Xu, F., Zhang, K. & Grunstein, M. (2005). Acetylation in histone H3 globular domain regulates gene expression in yeast. *Cell*, **121**, 375–385.
31. Chen, C. C., Carson, J. J., Feser, J., Tamburini, B., Zabaronek, S., Linger, J. & Tyler, J. K. (2008). Acetylated lysine 56 on histone H3 drives chromatin assembly after repair and signals for the completion of repair. *Cell*, **134**, 231–243.
32. Li, Q., Zhou, H., Wurtele, H., Davies, B., Horazdovsky, B., Verreault, A. & Zhang, Z. (2008). Acetylation of histone H3 lysine 56 regulates replication-coupled nucleosome assembly. *Cell*, **134**, 244–255.
33. Celic, I., Verreault, A. & Boeke, J. D. (2008). Histone H3 K56 hyperacetylation perturbs replisomes and causes DNA damage. *Genetics*, **179**, 1769–1784.
34. Williams, S. K., Truong, D. & Tyler, J. K. (2008). Acetylation in the globular core of histone H3 on lysine-56 promotes chromatin disassembly during transcriptional activation. *Proc. Natl Acad. Sci. USA*, **105**, 9000–9005.
35. Xu, F., Zhang, Q., Zhang, K., Xie, W. & Grunstein, M. (2007). Sir2 deacetylates histone H3 lysine 56 to regulate telomeric heterochromatin structure in yeast. *Mol. Cell*, **27**, 890–900.
36. Watanabe, S., Resch, M., Lilyestrom, W., Clark, N., Hansen, J. C., Peterson, C. & Luger, K. Structural characterization of H3K56Q nucleosomes and nucleosomal arrays. *Biochim. Biophys. Acta*, **1799**, 480–486.
37. Andrews, A. J., Chen, X., Zevin, A., Stargell, L. A. & Luger, K. (2010). The histone chaperone Nap1 promotes nucleosome assembly by eliminating non-nucleosomal histone DNA interactions. *Mol. Cell*, **37**, 834–842.

38. Luger, K., Rechsteiner, T. J., Flaus, A. J., Waye, M. M. & Richmond, T. J. (1997). Characterization of nucleosome core particles containing histone proteins made in bacteria. *J. Mol. Biol.* **272**, 301–311.
39. Flaus, A., Luger, K., Tan, S. & Richmond, T. J. (1996). Mapping nucleosome position at single base-pair resolution by using site-directed hydroxyl radicals. *Proc. Natl Acad. Sci. USA*, **93**, 1370–1375.
40. Poirier, M. G., Oh, E., Tims, H. S. & Widom, J. (2009). Dynamics and function of compact nucleosome arrays. *Nat. Struct. Mol. Biol.* **16**, 938–944.
41. Tonjes, R. & Doenecke, D. (1985). Structure of a duck H3 variant histone gene: a H3 subtype with four cysteine residues. *Gene*, **39**, 275–279.
42. Marzluff, W. F., Gongidi, P., Woods, K. R., Jin, J. & Maltais, L. J. (2002). The human and mouse replication-dependent histone genes. *Genomics*, **80**, 487–498.
43. Roberts, S. B., Emmons, S. W. & Childs, G. (1989). Nucleotide sequences of *Caenorhabditis elegans* core histone genes. Genes for different histone classes share common flanking sequence elements. *J. Mol. Biol.* **206**, 567–577.
44. Villain, M., Vizzavona, J. & Rose, K. (2001). Covalent capture: a new tool for the purification of synthetic and recombinant polypeptides. *Chem. Biol.* **8**, 673–679.
45. Richmond, T. J. & Davey, C. A. (2003). The structure of DNA in the nucleosome core. *Nature*, **423**, 145–150.
46. Clegg, R. M. (1992). Fluorescence resonance energy transfer and nucleic acids. *Methods Enzymol.* **211**, 353–388.
47. Wan, Q. & Danishefsky, S. J. (2007). Free-radical-based, specific desulfurization of cysteine: a powerful advance in the synthesis of polypeptides and glycopolypeptides. *Angew. Chem. Int. Ed. Engl.* **46**, 9248–9252.
48. Koopmans, W. J., Buning, R., Schmidt, T. & van Noort, J. (2009). spFRET using alternating excitation and FCS reveals progressive DNA unwrapping in nucleosomes. *Biophys. J.* **97**, 195–204.
49. Kruihof, M. & van Noort, J. (2009). Hidden Markov analysis of nucleosome unwrapping under force. *Biophys. J.* **96**, 3708–3715.
50. Li, G., Levitus, M., Bustamante, C. & Widom, J. (2005). Rapid spontaneous accessibility of nucleosomal DNA. *Nat. Struct. Mol. Biol.* **12**, 46–53.
51. Wang, Z., Zang, C., Rosenfeld, J. A., Schones, D. E., Barski, A., Cuddapah, S. *et al.* (2008). Combinatorial patterns of histone acetylations and methylations in the human genome. *Nat. Genet.* **40**, 897–903.
52. Ferreira, H., Flaus, A. & Owen-Hughes, T. (2007). Histone modifications influence the action of Snf2 family remodelling enzymes by different mechanisms. *J. Mol. Biol.* **374**, 563–579.
53. Adkins, M. W., Howar, S. R. & Tyler, J. K. (2004). Chromatin disassembly mediated by the histone chaperone Asf1 is essential for transcriptional activation of the yeast PHO5 and PHO8 genes. *Mol. Cell*, **14**, 657–666.
54. Dechassa, M. L., Zhang, B., Horowitz-Scherer, R., Persinger, J., Woodcock, C. L., Peterson, C. L. & Bartholomew, B. (2008). Architecture of the SWI/SNF–nucleosome complex. *Mol. Cell. Biol.* **28**, 6010–6021.
55. Friedberg, E. C. (2006). *DNA Repair and Mutagenesis*, 2nd edit. ASM Press, Washington, DC.
56. Javaid, S., Manohar, M., Punja, N., Mooney, A. M., Ottesen, J. J., Poirier, M. G. & Fishel, R. (2009). Nucleosome remodeling by hMSH2–hMSH6. *Mol. Cell*, **36**, 1086–1094.
57. Schnolzer, M., Alewood, P., Jones, A., Alewood, D. & Kent, S. B. (1992). *In situ* neutralization in Boc-chemistry solid phase peptide synthesis. Rapid, high yield assembly of difficult sequences. *Int. J. Pept. Protein Res.* **40**, 180–193.
58. Blake, J. (1981). Peptide segment coupling in aqueous medium: silver ion activation of the thiolcarboxyl group. *Int. J. Pept. Protein Res.* **17**, 273–274.
59. Hackenberger, C. P. (2006). The reduction of oxidized methionine residues in peptide thioesters with NH4I–Me2S. *Org. Biomol. Chem.* **4**, 2291–2295.
60. Hackeng, T. M., Griffin, J. H. & Dawson, P. E. (1999). Protein synthesis by native chemical ligation: expanded scope by using straightforward methodology. *Proc. Natl Acad. Sci. USA*, **96**, 10068–10073.
61. Luger, K., Rechsteiner, T. J. & Richmond, T. J. (1999). Preparation of nucleosome core particle from recombinant histones. *Methods Enzymol.* **304**, 3–19.
62. Little, J. W., Kim, B., Roland, K. L., Smith, M. H., Lin, L. L. & Slilaty, S. N. (1994). Cleavage of LexA repressor. *Methods Enzymol.* **244**, 266–284.
63. Thastrom, A., Lowary, P. T. & Widom, J. (2004). Measurement of histone–DNA interaction free energy in nucleosomes. *Methods*, **33**, 33–44.